

Liquid water on Mars

Ron L. Levin^{*a}, John L. Weatherwax^{*b}

^a46 Washington Avenue, Burlington, MA USA 01803

^b28B Bigelow Street, Cambridge, MA 02139

ABSTRACT

Key to the possibility of Martian biology is the availability of liquid water. The issue hinges on the physics of water under an atmosphere whose total pressure is only slightly higher than the triple point of water. The general consensus, that liquid water cannot exist on the Martian surface, was first challenged¹ in 1998. This paper offers a more detailed analysis.

While orbital images from Mariner 9 onward have shown evidence of ancient water flows, recent Global Surveyor and Odyssey orbiters have produced images of apparently active erosion. The 1997 Pathfinder Lander measured surface atmospheric temperatures well above freezing, while temperatures one meter higher were as low as -40° C. The low vapor capacity of the atmosphere just above the surface acts as a lid, or barrier, to evaporation. This could allow ice to melt into liquid water instead of subliming to vapor. In 2000, in a demonstration² made in a simulated Martian environment, water ice melted and remained liquid. However, many questions have been raised about the physics of this experiment. In this paper, numerical simulation provides values for the thermodynamic quantities controlling the phase of water. The binary diffusion coefficient of water vapor in CO_2 , and the law of binary gas diffusion are applied. Fluxes of water vapor under Martian conditions, including wind speeds, are calculated for various distances from surface ice sources. Evaporative heat loss is compared to the heat available from the sun. The paper provides the theoretical, if counterintuitive, basis for the existence of liquid water on the present Martian surface.

Keywords: water on Mars, liquid water on Mars, surface water on Mars, life on Mars, Mars environment

1. INTRODUCTION

Since the Viking Mission, the search for extinct and extant life on Mars has largely centered around the availability of liquid water on the surface of Mars at present and in the past. It is commonly believed that liquid water is a requirement for the existence of microbial life on Mars³. The discovery of microbial life on Mars would contribute significantly to the understanding of life's origin, variability, and the capability of its propagation through space.

Over the last several years, various findings have indicated the presence of water on or near the surface of Mars. Each of the two currently operating Mars orbiters has shown evidence for water in some form on the surface of Mars.

In 1998⁴, the Mars Global Surveyor satellite showed images of erosion gullies along the sides of steep cliffs on Mars that, according to geologists, are no older than a million years. This is evidence of very recent, if not current, water on the surface of Mars, perhaps in liquid form. Some scientists⁵ have suggested alternative explanations for these gullies such as flows of dry ice or slurries not involving liquid water.

Another recent indication of water on the surface of Mars comes from the Mars Odyssey orbiting spacecraft, which carried onboard a detector (GRS) capable of counting the flux of epithermal neutrons from the surface⁶. Epithermal neutrons result from cosmic rays striking the surface. The high energy cosmic rays give rise to high energy neutrons, which are thermalized to epithermal neutrons of more moderate energies if hydrogen is present. The GRS shows large percentages of hydrogen, assumed to be water, within the top meter of the soil, the limit of its sensitivity. As much as 30% water by mass was detected. Some of this water could be at the surface because the GRS experiment is not sensitive to the depth profile of the water within the top meter. The phase of the water would be subject to the temperature at any specific site.

*Currently working at MIT Lincoln Laboratory: e-mail ronlevin@comcast.net; phone 781-272-1497; fax 781-272-1497.

The Mars Odyssey also carried an infrared experiment, THEMIS, that could measure temperatures at the surface⁷. These temperature measurements show that, at the more moderate latitudes, daytime temperatures exceed 0°C. It has been shown⁸ that, by overlaying the GRS map with the infrared map of temperature from THEMIS, there is a great deal of hydrogen, presumed as water, even in latitudes near the equator, areas that at times exceed 0°C. These experimental results support the possibility of liquid water being available at the surface. However, to many, the possibility of liquid water existing under an atmosphere only 40% greater than the triple point pressure of water seems counter-intuitive.

In this paper, computer simulation of ice, liquid water, and water vapor on the surface of Mars under an atmosphere of 10 mb total pressure provides a complete, in-depth understanding of the thermodynamic balance. Quantities that can be extracted from the simulation include the rate of evaporation, the heat loss caused by this evaporation, the partial pressure of water at all locations, and the rate at which water vapor is being evolved from any ice or liquid water present.

This simulation was first motivated by an observation of a sustained 273°C soil temperature made by the Viking Lander 2 in 1976⁹. Near the lander, a large amount of snow or frost was seen lasting up to 200 days (Figure 1). Visual inspection of this image indicates at least 1-2 mm of snow or frost depth. The image also shows patches of this ice that are at least a square meter in area. This observation forms an important input to the simulation.

2. SPHERICAL MODEL

The simplest model places the ice or water on the surface of a sphere. The sphere of ice or water is suspended in an infinite, uniform atmosphere, with Martian sunlight impinging equally at all points of the sphere at the flux and intensity measured on Mars. This model reduces the problem to a single dimension, that of the distance away from the center of the sphere. Since wind breaks the spherical symmetry and reduces the cylindrical symmetry, its effects will be omitted here, but discussed later in the paper.

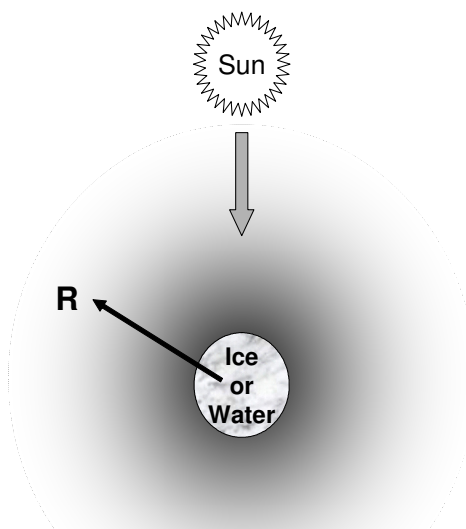
The other assumptions are shown in Figure 2. The partial pressure of water immediately surrounding the sphere is determined by the temperature of the sphere. A fast, thermodynamic equilibrium occurs between the ice or liquid phase and the vapor immediately adjacent. The rest of the model is based on the rate at which water vapor diffuses away from the sphere. This depends on binary diffusion, the diffusion of one gas through another. For purposes of this model, the two gases are water vapor and carbon dioxide. As fast as the water diffuses away from the immediate surroundings of the sphere, it is replaced by new water vapor evaporating from the ice or water. The rate of evaporation is thus controlled by the speed at which water vapor diffuses away from this spherical surface.

Figure 2: Spherical Model for Evaporation of Ice or Water

With spherical symmetry the problem has one dimension: **R**

Assumptions:

- Suspended Sphere of Ice (or Water)
 - Uniform radius
 - Uniform temperature
- Atmosphere
 - Infinite and uniform
 - Pure CO₂
 - No other sources of humidity
 - 10 mb total pressure
 - No wind
- Solar Illumination
 - Uniform around ice (or water) sphere
 - Constant in time
 - $\leq 500 \text{ w/m}^2$



Because this model has been greatly simplified and exists in only one dimension, it is possible to solve for the evaporation rate and to model all properties of this process with analytical equations. Equation 1 is Fick's First Law of Diffusion for steady state processes.

$$\text{Eq. 1} \quad \nabla^2 C_{\text{Water}} = 0$$

This law states that the Laplacian of the distribution of water vapor must be 0 everywhere, except at the surface, where there is a boundary condition. Equation 2 shows the same equation where spherical symmetry is assumed.

$$\text{Eq. 2} \quad \frac{d}{dr} \left(r^2 \frac{d}{dr} C_{\text{Water}} \right) = 0$$

Equation 3 shows the solution to this differential equation.

$$\text{Eq. 3} \quad C_{\text{Water}}(r) = C_{\text{Water}}(R) \frac{R}{r}$$

The concentration of water vapor is subject to a $1/r$ distribution that decreases with increasing distance from the sphere. The boundary condition at the surface of the sphere requires that, when the radial distance is equal to the radius of the sphere (R), the concentration of water vapor must equal that required by the evaporation equilibrium.

The flux of water vapor diffusion can now be written in closed form, and this current of water vapor is shown in Equation 4. The current has a $1/r^2$ distribution.

$$\text{Eq. 4} \quad j = -D \nabla C_{\text{Water}} = DC_{\text{Water}}(R) \frac{R}{r^2} \hat{r}$$

Equation 5 shows the integrated total outward flux of water vapor, which is the integral over any Gaussian surface enclosing the sphere.

$$\text{Eq. 5} \quad 4\pi R D C_{\text{Water}}(R)$$

The surface shape does not matter as long as the sphere is completely contained within this closed surface. The result shows that the total flux depends on the concentration of water at the surface of the sphere, which depends on the temperature, the diffusion coefficient, and the radius of the sphere.

Equation 6 shows the total flux per unit area at the surface of the sphere. The outward loss of water per unit area is proportional to $1/R$, where R is the radius of the sphere.

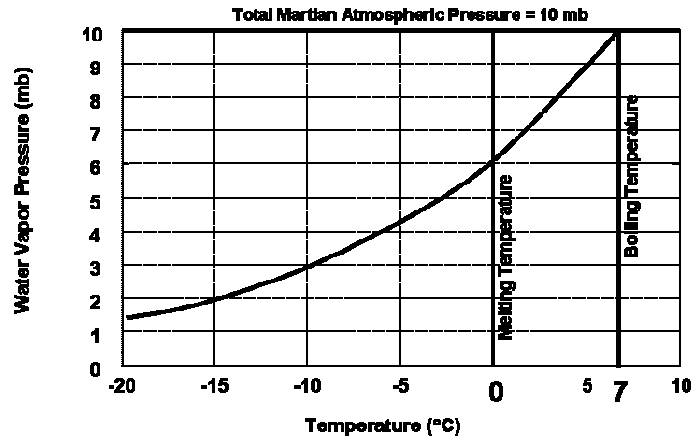
$$\text{Eq. 6} \quad \frac{D C_{\text{Water}}(R)}{R}$$

The larger the radius of the sphere, the more slowly water will evaporate. This is because, in a large sphere, a great deal of evaporating water vapor is competing for the same atmosphere in the immediate vicinity. This inhibits the escape of the vapor. The value¹⁰ for the heat of sublimation, in which ice passes directly to water vapor, is 2596 Joules per gram. This value is very close to that of the heat of vaporization. The flux per unit area can be turned into heat loss per unit area by multiplying the flux by the heat of sublimation.

To complete the model, it is necessary to look up the steam table data¹¹ on the partial pressure of water immediately in the vicinity of ice or water as a function of temperature. The relevant portion of this curve is shown in Figure 3.

This curve shows the vapor pressures for temperatures from -20°C to $+7^\circ\text{C}$. Across this range of temperatures, the vapor pressure of water rises from $1\frac{1}{2}$ millibars to 10 millibars. The boiling point for water on the surface of Mars is 7°C . The concentration of water vapor in the atmosphere is directly proportional to partial pressure of water and may be calculated

Figure 3: Water Vapor Pressure at the Surface of the Ice or Water



from the ideal gas law. The concentration of water vapor rises quite rapidly as a function of temperature. This means that the rate of evaporation increases strongly with the temperature. At the melting point 0°C, the partial pressure of water vapor is 6.1 millibars, the so-called triple point pressure (compared to 10 millibars total pressure).

Immediately adjacent to any liquid water or ice melting into liquid water, the atmosphere must be at least 6.1/10, or approximately 60% water vapor and only 40% CO₂. Water at a temperature greater than 0°C has an even higher concentration of vapor immediately adjacent to it. The transport of water vapor away from the immediate vicinity of the sphere is controlled by the binary diffusion coefficient for the gases carbon dioxide and water vapor. Although Berezhnoi and Semenov¹² provide a large number of binary diffusion coefficients between CO₂ and a variety of gases, the binary diffusion coefficient for water with carbon dioxide is not listed. It was, therefore, calculated.

Table 1 provides a matrix of values surrounding the desired value for water and carbon dioxide. A least squares fit in the dimensions shown provides the best value for the binary diffusion coefficient between water and carbon dioxide: 1.53 times 10⁻⁵ m²/sec, at room temperature and pressure. The book lists a correction formula that permits converting the binary diffusion coefficient from room temperature and pressure to that of Martian temperature and pressure. The most important correction is that for atmospheric pressure, 100 times lower on Mars than on Earth, raising the binary diffusion coefficient by a factor of 100. The temperature change provides a minor correction. The net result is a binary diffusion coefficient of 1.33 x 10⁻³. This formula is shown in Equation 7.

Table 1: Binary Diffusion Coefficients

	H ₂	He	N ₂	CO ₂
Water	88.5	84.5	25.3	15.3
Methyl Alcohol	61		16.9	10.4
Ethyl Alcohol	46.5	49.9	13.6	8.2
Propyl Alcohol	38	35	10.5	7.1
Butyl Alcohol	32	26	8.5	5.5

x 10⁻⁶

Eq. 7
$$D(P,T) = D_0 \left(\frac{P}{P_0} \right)^{-1} \left(\frac{T}{T_0} \right)^{1.5} = 15.3 \times 10^{-6} \left(\frac{10 \text{ mb}}{1000 \text{ mb}} \right)^{-1} \left(\frac{273 \text{ K}}{300.15 \text{ K}} \right)^{1.5} = 1.33 \times 10^{-3}$$

3. SPHERICAL MODEL RESULTS

With all constants determined, this analytical model can now generate numeric results. Figure 4 (using the left-hand scale) shows the rate of sublimation in mm/hr. This is calculated at different temperatures for the ice or water if the temperature is above 0°C, and for differing surface areas. The larger the surface area of the ice, the more slowly it

sublimes. The higher the temperature, the more rapidly ice sublimes. For 10^{-3} m^2 ice surfaces at 0°C , ice can sublime at the rate of a millimeter of depth per hour. For a one square meter patch of ice at 0°C , the sublimation rate is approximately 0.1 mm/hr. This sublimation rate can be converted into a flux of evolved gas at the surface of the sphere as can be seen on the center scale in Figure 4. For ice surfaces as small as 10 cm^2 , the velocity of the flux can be as high as 1 cm/sec.

More important than these calculations are the ones for evaporative heat loss also shown in Figure 4 on the right-hand scale. The color indicates the evaporative heat loss per unit area under each condition. These calculated values range from approximately 1/3 of a watt per square meter to $3,000 \text{ w/m}^2$. At 0°C , for a surface area of ice of one m^2 , the evaporative heat loss is approximately 60 w/m^2 . This is much less than the maximum solar flux that could be received on Mars of 500 w/m^2 ¹³. A line is drawn on this figure at 0°C , the melting temperature of ice and along the contour of 500 watts per square meter. The upper right hand portion of this plot shows conditions under which liquid water exists. Anywhere in this region it is possible for the energy provided by the sun to equal or exceed the energy lost by evaporation and, thus, be able to maintain the water at a temperature above 0°C .

This observation shows that for larger areas of ice, underneath bright sunlight, the temperature can be raised above 0°C since the Sun's heat input can exceed heat lost due to evaporation. Another way of showing this is by plotting the equilibrium temperature of the ice or liquid water under varying amounts of solar illumination. This equilibrium temperature is defined as the temperature at which heat loss from evaporation would equal heat gain from solar illumination. This result is shown in Figure 5. The solar flux in w/m^2 starts at 0 and goes up to 500, the maximum possible on Mars. The color indicates the equilibrium temperature. Dark blue is -25°C and bright red is 7°C , the maximum possible equilibrium temperature.

At 7°C , water boils on Mars and, therefore, the evaporative heat loss will be whatever is necessary to remove all the solar input if the temperature tries to exceed 7°C . Almost half of this plot shows an equilibrium temperature at the boiling point. The equilibrium temperatures for all solar fluxes are calculated.

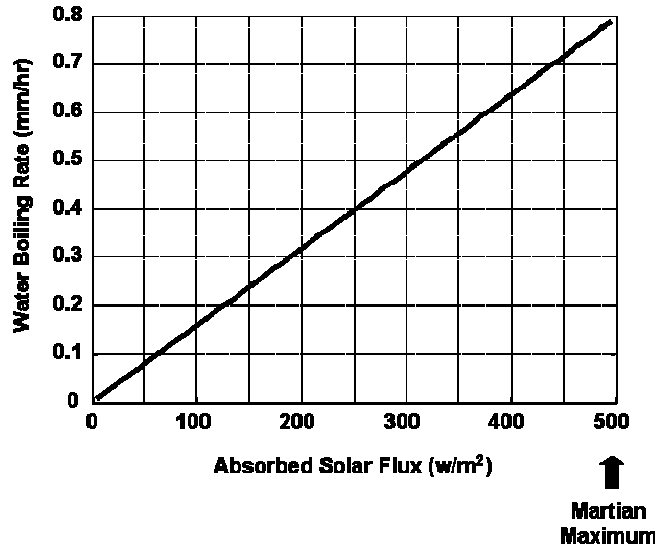
The lower white contour line is for 0°C . Equilibrium temperatures above this 0° contour indicate liquid water. The upper contour line is for 7°C . All conditions above this contour indicate boiling water, a mixture of liquid with steam arising. Eventually all water would boil away. In other locations on this plot, all water or ice would eventually evaporate, but that equilibrium would take hours to achieve. In the meantime, the equilibrium condition is divided into three results: solid ice, liquid water, and boiling water.

Two dotted vertical lines are shown on this plot. They represent the amount of sunlight that would be absorbed if there were no atmospheric absorption and the incident surface directly faced the sun. The line at 100 w/m^2 is for new snow, which has an absorption of 20%¹⁴. The vertical line at 350 w/m^2 is for old snow. It is important to remember that these absorption figures could be lower if the atmosphere absorbs to an appreciable extent, or if the incident angle of sun is not perpendicular.

Important limits on the solar absorption in the atmosphere can be determined by examining experimental data from the power output of the Mars Pathfinder solar cells. The efficiency of these solar cells is well known, as is the angle of sunlight incident upon them. The data for their power production can be used to estimate the absorption by the atmosphere. Figure 6 shows the boiling rate for water at Martian pressure of 7°C . When water is boiling, the rate of water dissipation will be the amount necessary to dissipate the heat provided. The absorbed solar flux divided by the heat of vaporization provides the depth of water that would boil away from a surface. This is independent of the size or the surface area of the water.

Liquid water on the surface of Mars receiving the maximum possible sunlight would boil away at the rate of 0.8 mm/hr. The spherical model indicates that, for the size of snow patches seen in the Viking Lander 2, an illumination of only 100 w/m^2 is probably sufficient to cause melting into liquid if no wind were present. This spherical model is conservative because it is the most favorable geometry for evaporation. If the ice surface were distributed on a flat plain instead, there would be a slightly reduced volume of atmosphere adjacent or in the near vicinity to absorb the water vapor, and evaporation would be reduced, increasing the prospects for liquid water.

Figure 6: Water Boiling Rate at 7°C



4. CYLINDRICAL MODEL WITH SIMULATED UNIFORM WIND

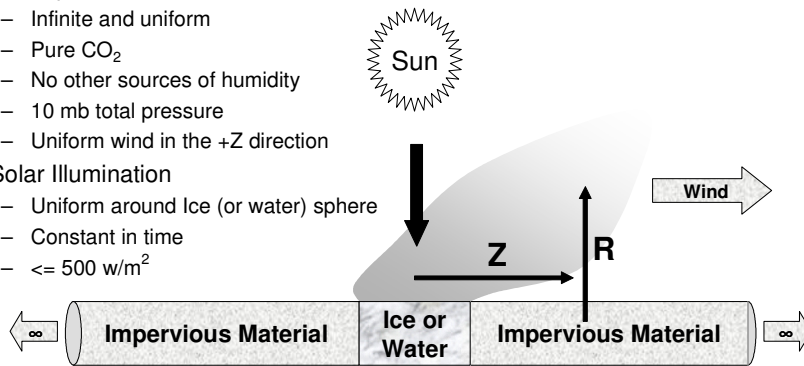
A more realistic simulation of evaporating ice on the surface of Mars is shown with a cylindrical model. This permits introduction of the effect of wind. Wind increases evaporation by transporting water vapor away from the area of evaporation, causing the ice or liquid to replace the vapor more rapidly. In effect, the wind is a mechanism for distributing the water vapor to a larger volume of air more rapidly. The concept behind this simulation is shown in Figure 7.

Figure 7: Cylindrical Numeric Model for Evaporation of Ice or Water

With cylindrical symmetry the problem has two dimensions: R & Z

Assumptions:

- Suspended Cylinder Ice (or Water)
 - Uniform temperature
 - Ends of cylinder connect to an infinite cylinder of solid material
- Atmosphere
 - Infinite and uniform
 - Pure CO_2
 - No other sources of humidity
 - 10 mb total pressure
 - Uniform wind in the $+Z$ direction
- Solar Illumination
 - Uniform around Ice (or water) sphere
 - Constant in time
 - $\leq 500 w/m^2$



An infinitely long impervious cylinder of radius R is envisioned, in which a small, segment has been replaced by ice or water. A constant uniform wind is blowing in the direction of the length of the cylinder. This provides a smooth, laminar flow, moving at constant velocity along the cylinder. Calculations can then be made at a variety of simulated wind speeds. All other assumptions are listed in this figure.

This problem now becomes a two-dimensional one, with both a radial dimension, R, away from the cylinder and a Z dimension along the cylinder in, or against, the direction of the wind. Equation 8 shows the steady state law of diffusion in the cylindrical geometry with the two variables R and Z.

$$\text{Eq. 8} \quad \frac{d^2}{dr^2} C_{water} + \frac{1}{r} \frac{d}{dr} C_{water} + \frac{d^2}{dz^2} C_{water} = 0$$

Because under the boundary conditions, this equation cannot be readily solved in closed form, this partial differential equation will be solved numerically on a discretized grid above the cylinder. The current of water vapor in this cylindrical geometry is shown in Equation 9.

$$\text{Eq. 9} \quad j = -D \left[\frac{\partial}{\partial r} \hat{z} + \frac{\partial}{\partial z} \hat{r} + V_{wind} \hat{z} \right] C_{water}(r, z)$$

This permits conversion of the solution for the concentration of water vapor from the numeric model into a numeric model for the flux of water vapor. Equation 10 shows the total output of water vapor numerically integrated over a Gaussian surface completely enclosing the water or ice.

$$\text{Eq. 10} \quad \int_{Surface} j \cdot \hat{n} ds$$

Equation 11 shows this total flux divided by the total surface area of the ice or water.

$$\text{Eq. 11} \quad = \frac{\int_{Surface} j \cdot \hat{n} ds}{Surface Area}$$

This total calculated flux of water vapor is multiplied by the “heat of sublimation” (2596 J/g) to produce the simulated heat loss.

5. CYLINDRICAL MODEL RESULTS

Figure 8 illustrates the simulation for two conditions: one in which the wind speed is 0 and one in which the wind speed is 1 cm/sec. An illustration of the cylinder (and ice) is shown along the horizontal axis at the bottom of the figure. Above this cylinder is shown the calculated partial pressure of water. Red represents high partial pressures (near 6 mb), while blue represents low partial pressures (just above 0 mb).

In the top plot, the distribution falls off radially with distance. The contours are not exactly circular, because the R dimension, the radial distance away from the cylinder, takes the place of two dimensions, R and the angular polar coordinate; the latter not shown. At increasing ranges away from the cylinder, there is more atmosphere available to absorb the vapor than there is at increasing longitudinal distance, Z. The contours, instead of being perfectly circular are thus somewhat flattened on the top.

In the bottom plot a wind speed is introduced. The symmetry of the solution is destroyed, and the vapor cloud shows a strong preference in the downwind direction, very gradually dissipating. Still, according to the calculation, 0.1 mb of vapor pressure can be seen as far as 20 m downwind.

This calculation was performed as a set of simultaneous linear equations represented in an enormous, sparse matrix. The differential equation for the law of diffusion is represented at each pixel by a relationship between that pixel and five of its neighbors. Each pixel considers the pixel above, below, left, and right of its own location, and it also considers a pixel two elements downwind from its original location. This is known as the “second order upwind finite difference method.” It is necessary for numeric stability when the wind advection is to be modeled¹⁵.

In the general volume of the calculation, the differential calculation previously discussed is reduced to a linear equation among these six pixels, the central pixel and its five neighbors. Each pixel in the simulation provides an additional linear equation tying together itself and its five neighbors. Therefore, a linear equation exists for each pixel in the simulation. These linear equations are arranged in a square, sparse matrix where the horizontal and vertical dimensions are each the size of the number of pixels in the entire simulation. For example, if this two dimensional simulation included a volume of 256 longitudinal pixels and 256 radial pixels, the entire simulation would consist of 65,000 pixels. This would require a matrix that was 65,000 by 65,000 elements or 4.3 billion matrix elements. Fortunately, only about 400,000 elements are non-zero.

The differential equation at the edges of the simulation is modified to take into account the boundary conditions. Along the top, and the left and right edges, the boundary condition is that the vapor pressure should be equal to the average vapor pressure on Mars, which for this calculation was taken to be 0. Therefore, the differential equation solution will be 0 on the left, right, and top of this simulation. On the bottom of the simulation, over the portion where the ice or water exists, the partial pressure of water is set to the value derived from the steam table based on the surface temperature of that ice or water.

Along the rest of the cylinder, the boundary condition states that water vapor will neither be diffusing into, or out of, the cylinder, which means that the component of the gradient of water vapor normal to the surface of the cylinder must be 0. With that boundary condition and the others just discussed, the complete set of linear equations for all pixels is defined. Their coupled linear equations represented in the matrix are solved by Gaussian Elimination. The result is a partial pressure of water vapor for each pixel, as shown in the Figure 8.

Both Viking and Pathfinder landers measured wind speed^{16,17}, showing that wind speeds were generally only a few km/hr. Wind speeds during the day were generally below 10 km/sec. The numeric model was run for wind speeds between 0 and 10 m/sec. The results in terms of evaporative heat loss are shown in Figure 9.

In this figure, the horizontal axis shows the wind speed, and the vertical axis shows the area of the cylindrical surface of the ice or snow. The color indicates the heat loss in terms of w/m^2 if the surface of ice were at $0^\circ C$. This plot shows evaporative heat losses between 1 and 10,000 w/m^2 . Two black contours show the evaporative heat losses for 500 w/m^2 and 100 w/m^2 . As can be seen, areas of ice of only a few m^2 have evaporative heat losses less than 100 w/m^2 , even at a wind speed of 10 m/sec.

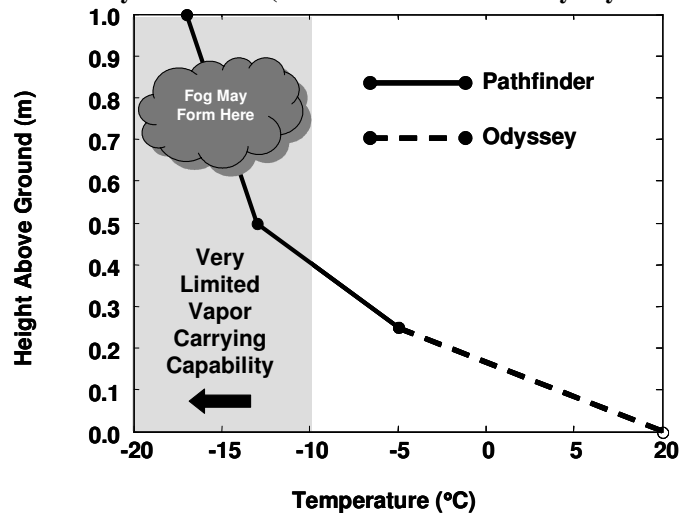
Another way of looking at this is to assume a value for the solar flux absorbed and ask what would the equilibrium temperature be for this ice/water mixture (when the evaporative heat loss exactly equals the insolation gain). The result is shown in Figure 10 for insolation values of 500 and 100 w/m^2 . On each plot, contours are shown in white for $0^\circ C$ and $7^\circ C$. These contours divide the plots into three regions, one in which the phase at the equilibrium is solid ice, one in which it is liquid water, and one in which it is boiling water. In the final analysis, the phase of water at the equilibrium temperature depends on the surface area, wind speed and solar insolation. In general, there are many regions in which the equilibrium temperature would result in liquid water.

6. THE MARTIAN COLD TRAP

Several factors that were not considered in these models could have a significant impact on the results. The most important of these is the presence of a "cold lid" just above the Martian surface¹⁸. Figure 11 shows data taken by the Pathfinder¹⁹ lander during the heat of the day and by the THEMIS experiment on Odyssey²⁰. It shows that temperatures below 1 meter above the ground rise dramatically. The temperature of the soil at the surface is even higher based on the THEMIS infrared measurements, rising to $20^\circ C$, or more.

This temperature profile constitutes an inversion, as occurs on Earth at higher elevations, and reduces vertical convection in the Martian atmosphere. The density of air on Mars is much less than on Earth, making the forces caused by differential densities correspondingly smaller; therefore, there is a much lesser tendency for warm air to rise. Also, the gravity on Mars is only 3/5 of that on Earth, which further reduces the differential forces that cause hotter, less dense air to rise.

Figure 11: Evaporation Limited by a Cold Lid (Mars Pathfinder and Odyssey THEMIS Temperature Data)



Because convection is so much weaker on Mars than on Earth, the drop off in temperature with altitude is much more severe. Although the temperature at the surface can reach 20°C, the temperature at 1 m altitude may be -15°C. Above 1 m is probably always sub-freezing.

According to the steam tables²¹, at -15°C, the atmosphere can hold no more than 2 mb partial pressure of water vapor. This means that water evaporating from the surface or ice sublimating can send water vapor sideways or even downwind, but cannot send water vapor in the vertical direction. This especially retards evaporation from liquid water or ice on the surface. Since nearly all geographic locations appear rich in near-surface ice, the horizontal dimension is effectively homogeneous, and the vertical becomes more important.

The Pathfinder data show that the ability to transport water vapor in the vertical direction is greatly limited and that most of the water vapor on Mars would have to exist within the 1 meter of atmosphere closest to the surface. This indicates that, if liquid water did form on Mars, or if areas of ice approached 0°C and began evaporating rapidly, that there is a great chance of fog forming at an altitude above the evaporation. This fog is often seen in pictures of the surface of Mars taken from Mars orbit²². Fog is especially prevalent in low valleys or depressions on Mars. Fog layers are regions in which the atmosphere is completely saturated with water vapor, where no further evaporation is possible. Ice (or water) under these conditions would not have any evaporative heat loss. Because of this, liquid water would exist if and when the ground temperature exceeds 0°C.

These findings support the experimental evidence for the existence of liquid water under simulated Martian conditions as demonstrated in a bell jar experiment, and in space suit porous plate backpack tests, both reported in 2000²³.

7. SUMMARY

In summary, numeric calculations show that ice on the surface of Mars may melt into liquid water under Martian solar illumination. Wind increases the rate of evaporation, but it is not as significant a factor as it might seem intuitively. This model allows examination of all the parameters surrounding a hypothesized area of evaporating ice or water. This study of the physics of evaporating water at 10 mb total pressure leaves some uncertainties as listed in Table 2. However, the combined effects seem likely to increase the probability for liquid water.

The ultimate conclusion is that there are no physical reasons prohibiting the availability of liquid water on the surface of Mars. This thermodynamic analysis provides evidence that biologically significant amounts of liquid water can currently exist on the surface of Mars. The previously presumed unavailability of liquid water is not a reason to rule out the existence of microbial life on current day Mars.

Table 2: Factors Not Modeled

Factor not Modeled	Qualitative Effect	Description
Cold Trap	Conservative	Atmospheric temperatures more than a meter above the surface are much colder than those at the surface. This reduces the amount of water vapor that the atmosphere can hold. Reduced vapor diffusion leads to reduced evaporation and makes the existence of liquid water more probable than was calculated.
Flat Ice Surface	Conservative	Spherical or cylindrical geometries modeled are more favorable for evaporation than the actual planar geometry of snow. This reduced evaporation makes liquid water more likely than was calculated.
Multiple Ice Patches	Conservative	The model assumes water vapor from a single patch is diffusing into an infinite dry atmosphere. The presence of nearby patches will increase the local humidity, reducing evaporation, making liquid water more likely than was calculated.
Dissolved Minerals	Conservative	Dissolved minerals (from the soil) lower the melting point of ice and reduce the sublimation rate. Both of these effects make liquid water more likely than was calculated.
Variability of Solar Heating	Unknown	No study was performed to calculate the amount of solar flux absorbed by ice as a function of time of day, orientation, latitude or season. Assumptions about the magnitude of solar heating could be in error in either direction, changing the conditions at which ice would melt into liquid water.
Heat Conduction	Unknown	Conduction (and to a lesser extent convection) can alter the heat balance used in these calculations. Conduction could absorb solar heat from near by rocks (usually darker than ice) and increase melting. Cold soil beneath the surface, however, might draw heat away from the ice. This unmodeled effect could change the likelihood of liquid water in either direction.
Wind Turbulence	Liberal	Wind turbulence (not modeled) increases the removal of water vapor and thus reduces the likelihood of liquid water. Turbulence in the model can be taken into account by increasing the wind speed above that measured by Mars landers.
Solar Attenuation	Liberal	Ice at temperatures near 0°C may send vapor up into the cold lid causing atmospheric condensation (fog). This fog will attenuate the sunlight that would otherwise heat the ice, making liquid water less likely than calculated.

ACKNOWLEDGMENTS

The authors gratefully acknowledge the suggestions, discussion, and review by Dr. Gilbert V. Levin, Viking Labeled Release Experimenter, and the superb word processing of Ms. Katherine Brailer, CEO and Executive Assistant, respectively, of Spherix Incorporated, Beltsville, Maryland.

REFERENCES

1. Levin, G.V. and R.L. Levin, "Liquid Water and Life on Mars," *Instruments, Methods, and Missions for Astrobiology, SPIE Proceedings*, **3441**, 30-41, July, 1998.
2. Levin, G., L. Kuznetz, and A. Lafleur, "Approaches to Resolving the Question of Life on Mars," *Instruments, Methods, and Missions for Astrobiology, SPIE Proceedings*, **4137**, 48-62, August 2000.
3. Huntress, Wesley, Jr., quoted in *The San Diego Union-Tribune*, p-A1, Feb. 19, 1998.
4. Malin, M.C. *et al.*, "Early Views of the Martian Surface from the Mars Orbiter Camera of Mars Global Surveyor," *Science* **279**, 1681-1685, 1988.
5. Costard, F., F. Forget, N. Mangold, and J. P. Peulvast, "Formation of Recent Martian Debris Flows by Melting of Near-Surface Ground Ice at High Obliquity," *Science* **5552**, 110-113, 2002.
6. Mitrofanov, I. *et al.*, "Maps of Subsurface Hydrogen from the High-Energy Neutron Detector, Mars Odyssey," *Science* **297**, 78-81, 2002.
7. Christensen, P.R. *et al.*, "Morphology and Composition of the Surface of Mars: Mars Odyssey THEMIS Results," *Science* **300**, 2056-2061, 2003.

8. Levin, G.V., "Odyssey gives evidence for liquid water on Mars," *Instruments, Methods, and Missions for Astrobiology VII, SPIE Proceedings*, in press.
9. Op Cit 1.
10. *Handbook of Chemistry and Physics*, 55th edition, pgs. B-244 and D-58, 1974-1975.
11. Op Cit 10, pg. D-159, 1974-1975.
12. Berezhnoi, A.N. and A.V. Semenov, "Binary Diffusion Coefficients of Liquid Vapors in Gases," *Begell House*, 1997.
13. Schuerger, A.C., R.L. Mancinelli, R.G. Kern, L.J. Rothschild, and C.P. McKay, "Survival of Endospores of *Bacillus subtilis* on Spacecraft Surfaces under Simulated Martian Environments: Implications for the Forward Contamination of Mars," *Icarus*, in press.
14. "Observations of Snow Cover from the Ground and Space," from the NASA Goddard Space Flight Center website, <http://snowcover.gsfc.nasa.gov/proc.albedo.html>.
15. Hirsch, C., "Numerical Computation of Internal and External Flows, Fundamentals of Numerical Discretization," John Wiley & Sons, 1990.
16. "Mars Pathfinder Preliminary Results," from the NASA Goddard Space Flight Center website, http://nssdc.gsfc.nasa.gov/planetary/marspath_results.html.
17. "Mars Pathfinder Windsocks," from the NASA Goddard Space Flight Center website, <http://mars.jpl.nasa.gov/MPF/ops/PR-windsocks.html>.
18. Op Cit 1.
19. Mars Pathfinder Mission Status, Jet Propulsion Laboratory, NASA, daily website reports, July 9 – August 1, 1997.
20. Brumby, S.P., D.T. Vaniman, and D. Bish, "Emissivity Spectrum of a Large "Dark Streak" from THEMIS Infrared Imagery," *Sixth International Conference on Mars*, 2003.
21. Op Cit 11.
22. Kiefer, W.S., A.H. Treiman, and S.M. Clifford, "The Red Planet: A Survey of Mars," *The Lunar and Planetary Institute*, a Universities Space Research Association publication, 1997.
23. Op Cit 2.

Figure 1: Some Patches of Frost/Snow, > 1 Square Meter

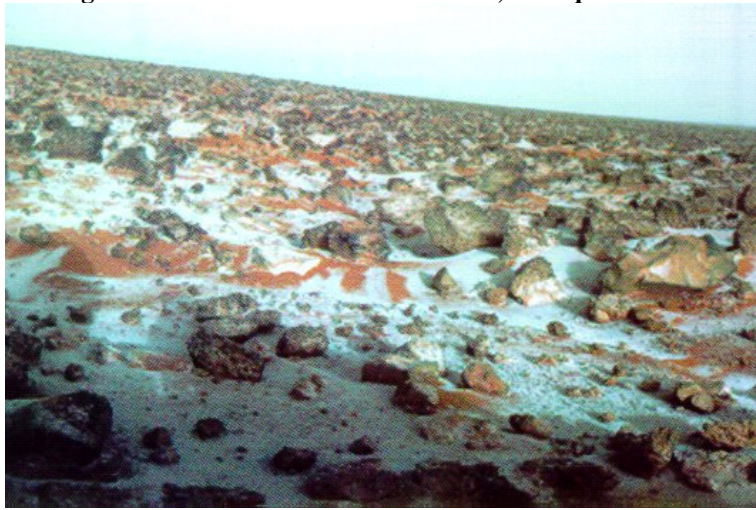


Figure 4: Ice Sublimation Rate, Evaporative Heat Loss, and Evolved Gas Speed

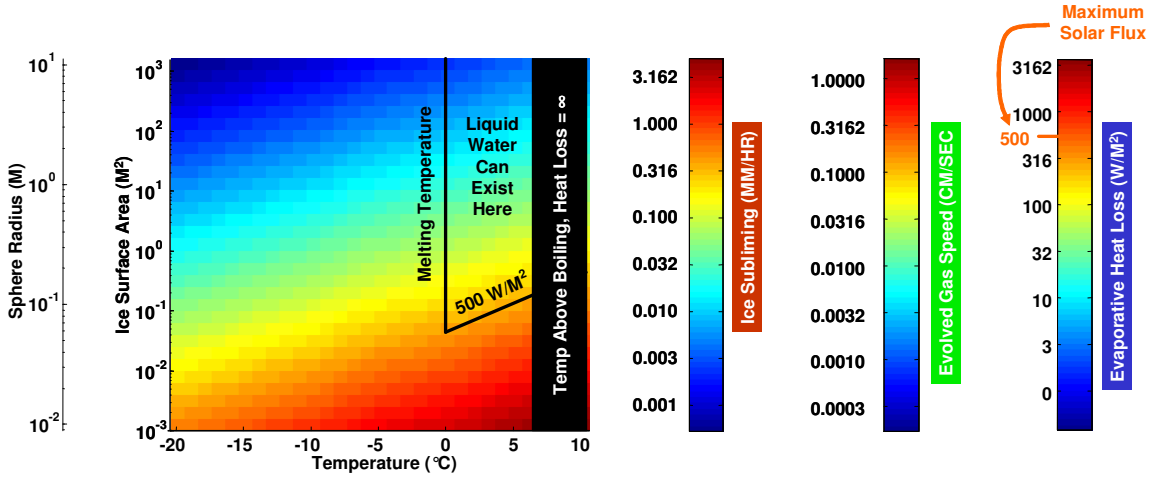


Figure 5: Phase of Water at Equilibrium Temperature

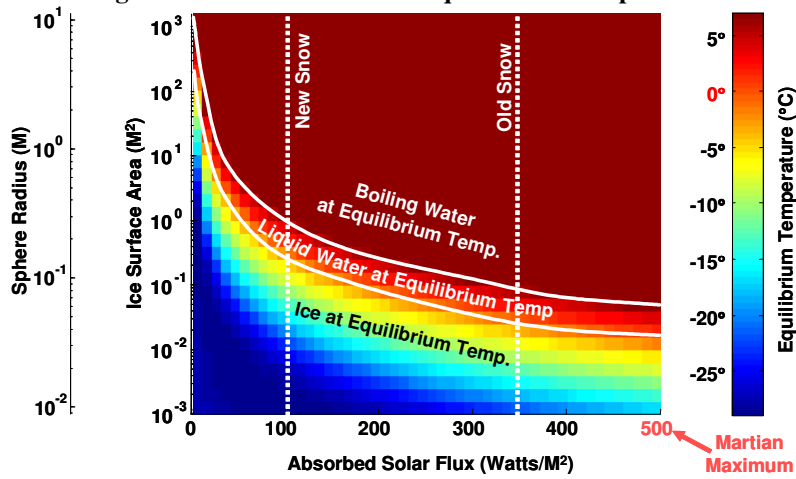


Figure 8: Vapor Pressure from Evaporating Ice or Water

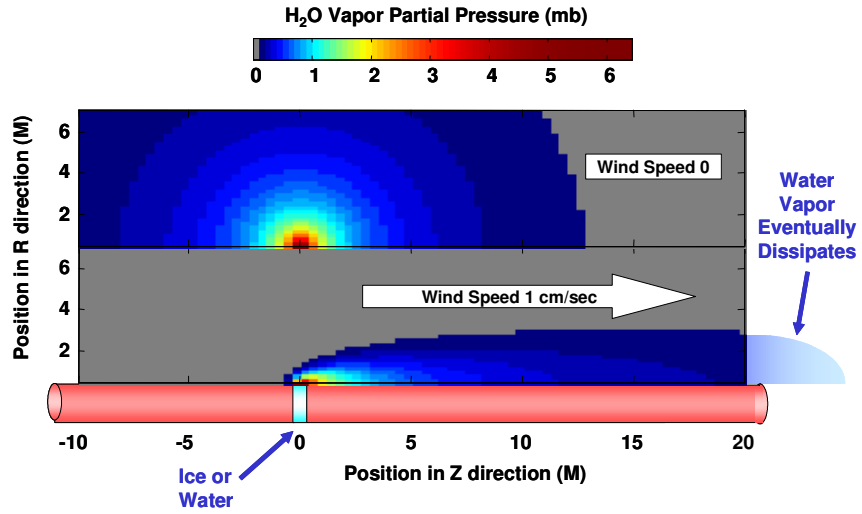


Figure 9: Evaporative Heat Loss at 0°C

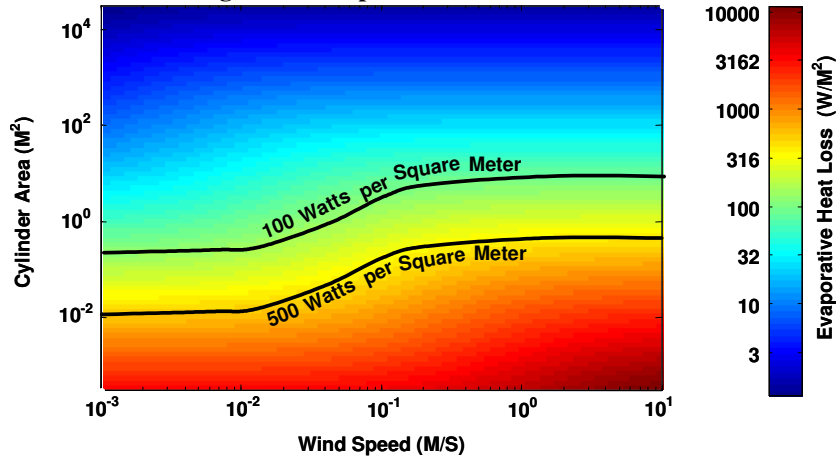


Figure 10: Equilibrium Temperature if Absorption is 500 Watts/M² or 100 Watts/M²

